Calculations of strain-modified anatase TiO_2 band structures

Lukas Thulin and John Guerra
Nanoptek Corporation, Maynard, Massachusetts 01754, USA
(Received 3 January 2008; revised manuscript received 21 April 2008; published 14 May 2008)

In order to theoretically quantify a strain-inducing method that we use to engineer the material properties of anatase titania, we studied its electronic band structure over a range of biaxial strain by utilizing both the density functional theory within the generalized gradient approximation (GGA) and quasiparticle theory calculations within the GW approximation. This strain-modified material is suitable for use as a high efficiency photoanode in a photoelectrochemical cell. We track the changes to the band gap and the charge carrier effective masses versus the total pressure associated with the strained lattice. Both the GGA and the GW approximation predict a linear relationship between the change in band gap and the total pressure. However, the GGA underestimates the slope by more than 57% with respect to the GW approximation result of 0.0685 eV/GPa. We also compare our predicted band gap shift to a reported experimental result.

DOI: 10.1103/PhysRevB.77.195112 PACS number(s): 71.15.Mb, 71.20.−b

I. INTRODUCTION

High efficiency photoelectrolysis for water splitting requires a photoelectrode with several basic properties that are difficult to embody in a single material. A catalytic material would ideally have[1] a band gap near 2.0 eV to absorb the maximum usable solar energy, an electron affinity that results in band edges that favorably align with the hydrogen reduction potential, a high charge carrier mobility to limit recombination, and stability within an aqueous environment. One such material that has received attention as a promising photoanode is the anatase polymorph of titanium dioxide. This material is among the best within the class of transition metal oxides that meets stability requirements, but its efficiency is too low, which is largely due to its wide band gap.[1,2] Doping has thus far been either unable to sufficiently reduce the band gap[3,4] or has detrimentally affected the other material properties needed for high efficiency.[5–7]

Here, we study the response of the anatase titania band structure to biaxial strain as an alternative method to alter its properties. In this instance, the most important property deducible from the band structure is the band gap. It is well known that the band gap of a semiconductor has a dependence on volume change, which is induced by either a temperature change or an applied force.[8] We have been working with nanostructured templates to impart high local stresses into titania thin films.[9] Moreover, we do not anticipate this mechanism of band gap reduction to increase the electron-hole recombination rate, considering the absence of point defects, which can be problematic when using dopants.[6] Another aspect relating to the efficiency is the effective mass of the charge carriers.[1,10] This quantity can be extracted from the curvature of the parabolic portions of the bands over a range in k space surrounding the conduction band minimum (CBM) or valence band maximum (VBM). A final material property to consider would be the alignment of the CBM and VBM with respect to the hydrogen reduction potential. A study of the band edge positions as a function of the lattice strain would require a series of slab models to calculate valid reference energies, and we will not consider it in this work. However, this type of study could be useful to reveal how the strain changes the need for an external bias voltage to split the water, which is an important factor in the maximum achievable efficiency.

The following sections are organized to detail the methodology, results, and conclusions of this work. Section II includes the energy cutoffs and other parameters that influence the accuracy of the density functional theory (DFT) and GW calculations, as well as a brief description of optimization and other calculation procedures. In Sec. III, we present the strain-induced changes to the band gap and charge carrier effective masses. Additionally, we compare the calculated results to an experimentally reported band gap shift achieved by this mechanism. Section IV estimates how the band gap reduction can be expected to increase the solar-to-hydrogen conversion efficiency of a photoelectrochemical cell.

II. METHOD

The calculations in this work have been done by using the ABINIT[11] package. ABINIT is a DFT implementation based on pseudopotentials and a plane wave basis set. ABINIT also goes beyond the DFT via the GW approximation, which is a tool that we require to accurately study the band gap.[12–15] In Sec. III, a comparison between the two methods will show that the generalized gradient approximation (GGA) is unable to accurately predict the derivative of the band gap with respect to the total pressure.

We used norm-conserving pseudopotentials from the Opium library[16] that incorporate the gradient corrected exchange-correlation functional of Perdew–Burke–Ernzerhof (PBE).[17] The oxygen pseudopotential includes the $2s$ and $2p$ states in valence, and the titanium pseudopotential includes the $3s$ and $3p$ semicore states, as well as the $3d$, $4s$, and $4p$ states in valence. The unoccupied $4s$ and $4p$ states in the titanium pseudopotential are included for transferability testing. A kinetic energy cutoff of 30.0 hartree for the plane waves demonstrated convergence of the forces and total energy. The Brillouin zone (BZ) sampling for the DFT calculations used a (4,4,4) Monkhorst–Pack[18] (MP) grid.

The GW calculation parameters were all determined through convergence studies with BZ sampling at Γ only

(excluding, of course, the convergence study of BZ sampling). The BZ sampling is safely reduced from 13 to 6 k points by using a (3,3,3) MP grid, which results in substantial savings in processing time while changing the GW band gap calculation by only 0.01 eV. Such high convergence also suggests that the change in the BZ sampling accuracy as a function of strain (due to the change in the BZ volume) is negligible. The cutoff energy was reduced to 25.0 hartree for the ground state portion of the GW calculations. For the screening calculation, we used 100 bands, a 12.0 hartree cutoff energy for the plane wave set representing the wave functions, and a 15.0 hartree cutoff for the plane wave set representing the dielectric matrix. The self-energy calculations required 150 bands, a 15.0 hartree cutoff for the plane wave set representing the wave functions, and an 18.0 hartree cutoff for the plane wave set used to generate the exchange part of the self-energy operator. The dimension of the screening matrix controls the correlation part of the self-energy operator.

To calculate the lattice parameters, we use a high (30.0 hartree) plane wave cutoff energy to ensure that the total pressure calculations are converged. The conventional unit cell of the anatase crystal is a body-centered tetragonal, which has two equal lattice constants a and a longer constant c. Therefore, by equal variation in the lattice constants a, followed by determination of the lattice constant c, the biaxial strain can be studied while conveniently maintaining the Bravais symmetry. For fixed a, we sample the total energy at five values of c; a quadratic fit to the data is then used to find c. Before each total energy calculation, the internal ionic coordinates are found by using the Broyden–Fletcher–Goldfarb–Shanno[19–22] (BFGS) minimization algorithm. The set of lattice constants that yield the minimum total energy are the theoretical equilibrium constants, and because of the high cutoff energy, also correspond to approximately zero pressure. After finding the optimum c/a ratio, we also fit the energy-volume data to a third-order Birch–Murnaghan[23] equation of state to calculate the bulk modulus. Here, we use the bulk modulus as an additional indicator of the transferability of the pseudopotentials.

Having ascertained the lattice constants for a set of strained lattices over a wide range of total pressures spanning approximately ± 10 GPa, we next proceed to the electronic band structure calculations for each lattice. Various references produce band structure plots that quite agree with ours.[24–26] Other references plot band structures along high symmetry lines suitable for a simple tetragonal lattice,[27–29] which makes direct comparison more difficult. As an aside, Asahi *et al.*[27] reported a conflicting result for the band gap type. These authors reported that the band gap type is marginally direct depending on the lattice parameters, whereas it is decisively indirect throughout our work. The source of this discrepancy is unclear and is not within the scope of this study. Our primary concern here is the influence it has on the penetration depth $(1/\alpha)$ of a semiconductor; the device design must consider this, given the obvious desire to promote the maximum absorption of the incident light.

The severe underestimation of the band gap is a well-known shortcoming of the DFT when using local approximations for the exchange-correlation functional.[30,31] Band structure calculations that produce results more consistent with experiment are possible with improved functionals[32] or the GW approximation,[12] although these methods are much more computationally time consuming. Often, and including a study of anatase titania by Calatayud *et al.*,[24] these improved methods find that the general characteristics of the band structures produced by local exchange-correlation functionals are reasonably accurate, barring the magnitude of the band gap. However, given that the primary goal of this work is to study the band gap, we elect to calculate it by using the GW approximation. We do use the DFT results to approximate the charge carrier effective masses.

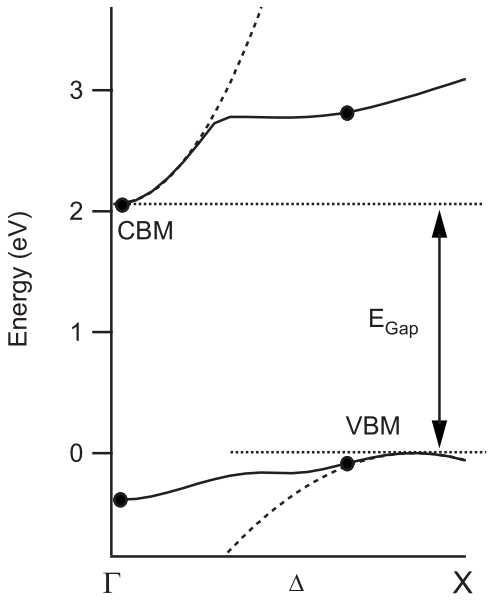

FIG. 1. Plot of the two bands containing the CBM and VBM along Δ. The effective mass calculations are based on the dashed curves. The minimum band gap is indirect with the CBM at Γ and the VBM at 0.86Δ. The solid points are indicators of where GW correction data are available.

The ABINIT implementation of the GW approximation presently restricts the correction to k points that are included in the MP grid from the self-consistent calculation. GW corrections at an arbitrary point are accomplished by appropriately shifting a grid so that it contains the point of interest. Only a very inefficient sampling grid can be found that contains the exact VBM, which is located at approximately 0.86Δ. The total computation time becomes unacceptable as it approximately follows the square of the number of k points.[11] Given this, we chose to calculate the GW correction at the two points shown in Fig. 1. Most important is the Γ point, which is the location of the CBM and is therefore the largest source of the GGA error. A nonshifted (3,3,3) grid contains Γ, as well as another point located at $2/3\Delta$, which is near the VBM and only 0.088 eV below it, and adds very little computational overhead to be included. We concluded that the VBM corrections at $2/3\Delta$, as opposed to those at 0.86Δ, easily track the minimum band gap to better than 5%.

The secondary measure of interest is the curvature of the parabolic portions of the bands near the CBM and VBM. The following simple relation[33] equates the curvature of the

bands to the effective mass of the electrons or holes:

$$m^* = \frac{\hbar^2}{2a}. \quad (1)$$

In Eq. (1), m^* is the effective mass of the charge carrier and a is the coefficient of the second order term in a quadratic fit of $E(k)$. Typical fitting results are plotted in Fig. 1.

III. RESULTS

The lattice optimization procedure described above yields theoretical values of $a=3.805$ Å and $c=9.781$ Å, which are overestimated by 0.61% and 2.93%, respectively.[34] The coordinates of the oxygen atoms are characterized by a third internal parameter u, which was determined after the BFGS minimization to be 0.2056 at equilibrium. The bulk modulus was found to be 184.5 GPa, which is very good compared to the experimental results of Arlt *et al.*[35] and Swamy and Dubrovinsky.[36] All parameters appear to be in good agreement with other gradient corrected pseudopotential plane wave (PP-PW) calculations, as seen in Table I.

The equilibrium lattice band structure is plotted in Fig. 2. The minimum indirect band gap of 2.054 eV along the Δ direction is in good agreement with other reported calculations, with the exception noted earlier. The GW calculations predict the equilibrium band gap between Γ and 2/3Δ to be 3.791 eV. This result is overestimated with respect to the experimental value of 3.2 eV but is very close to the 3.68 eV calculated by Calatayud *et al.*[24] by using the nonlocal B3LYP functional. Moreover, as discussed, our calculation is not precisely at the VBM, thereby overestimating the minimum band gap by a small amount.

Given that the absolute value of the band gap predicted by the GGA is not useful, it is interesting to investigate whether the GGA can accurately calculate the derivative of the band gap with respect to the total pressure. Both the GGA and the GW approximation predict this relationship to be linear (Fig. 3), but the slopes differ by such a large degree that the GGA results should be considered to be only qualitatively accurate. These slopes are predicted to be 43.51 meV/GPa by the GGA and 68.53 meV/GPa by the GW approximation. In this case, just as the GGA underestimates the absolute value of the band gap, it also underestimates its rate of change.

Simpson *et al.*[40] reported on the band gap shift of anatase titania strained by a lattice mismatched substrate. By using two different substrates that expand the lattice constant a by

TABLE I. Comparison of equilibrium parameters.

Source	Method	a (Å)	c (Å)	u	B_o (GPa)
	Experimental	3.782[a]	9.502[a]	0.208[a]	179[b]
Ref. 36	Experimental	3.791	9.515		178
This work	PP-PW-PBE	3.805	9.781	0.2056	184.5
Ref. 37	PP-PW-PBE	3.786	9.737	0.2056	176
Ref. 37	PP-PW-LDA	3.735	9.534	0.2069	199
Ref. 37	PP-PW-BLYP	3.828	9.781	0.2059	178
Ref. 24	AE-B3LYP	3.7723	9.9285	0.2028	200.34
Ref. 27	AE-FLAPW-LDA	3.692	9.471	0.206	
Ref. 25	AE-FLAPW-LDA	3.716	9.633	0.2081	
Ref. 29	PP-LCAO-HF	3.763	9.848	0.2020	
Ref. 38	AE-LCAO-HF	3.781	9.735	0.203	202
Ref. 39	INDO	3.641	9.197	0.203	

[a]Reference 34.
[b]Reference 35.

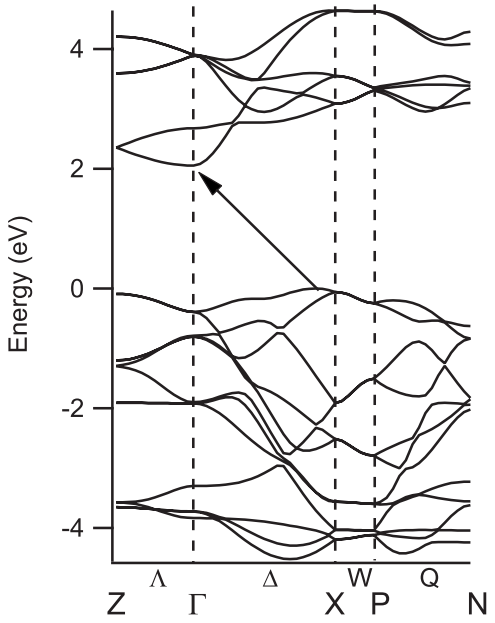

FIG. 2. Band structure plot for the equilibrium anatase TiO_2 lattice.

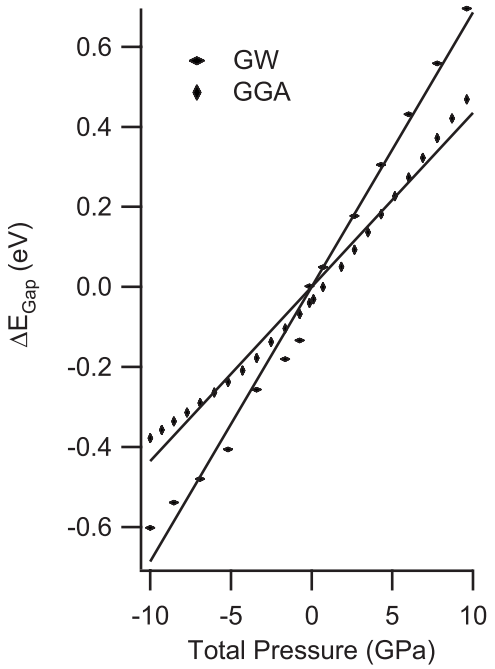

FIG. 3. Derivative of the band gap with respect to the total pressure. GGA and GW approximation results of the indirect gap between Γ and 2/3Δ.

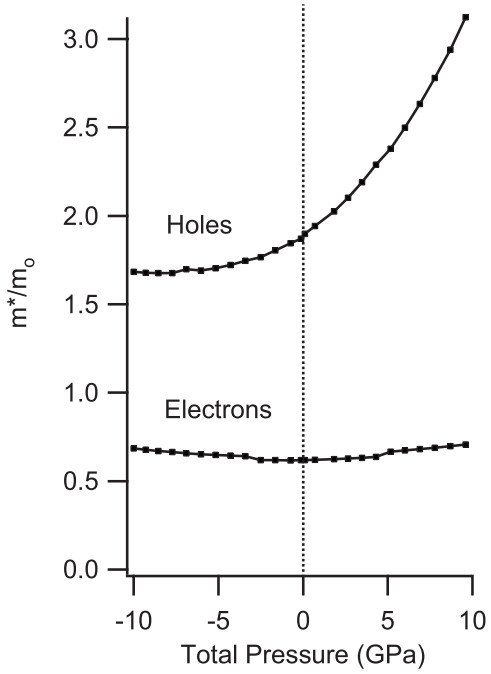

FIG. 4. Effective mass of the charge carriers vs the total pressure.

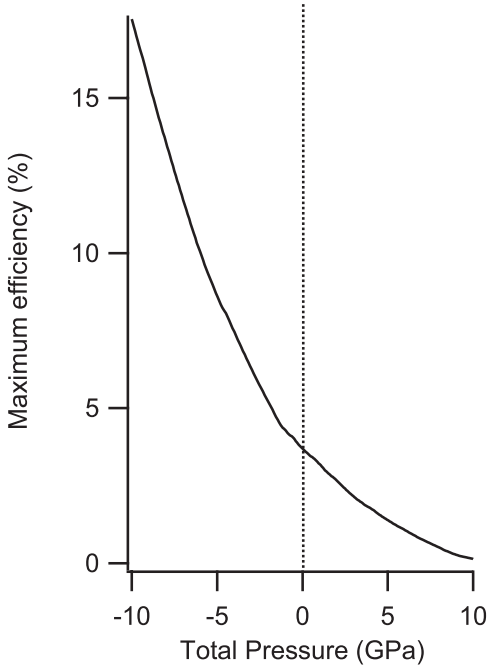

FIG. 5. Maximum achievable solar-to-hydrogen conversion efficiency vs total pressure.

0.2% and 1.5% (with respect to Ref. 34 equilibrium constants), these authors reported a 100 meV redshift in the band gap. When using the same strain percentages to a, our calculations predict a redshift of 153 meV. The difference is relatively large but within the experimental error.

Strain-induced alterations of the electron and hole effective masses are shown in Fig. 4. Interestingly, the calculations predict a minimum electron effective mass very near the equilibrium geometry so that the mass increases with either the tensile or the compressive strain. The electron effective mass for the equilibrium lattice is $0.62m_o$ within this primary valley; although we observed this calculation to be very sensitive to the curve fit. This serves as a partial indicator that the GGA calculations yield reasonable band variations given the experimental value[41] of $\sim 1.0m_o$. The overall strain dependence is very flat, which is a qualitative result that is sufficient for our purposes. The change in the effective mass of the holes is more pronounced and beneficial, with a non-negligible reduction in the mass with tensile strain. Therefore, the tensile strain may also increase the photon conversion efficiency by reducing electron-hole recombination.

IV. CONCLUSIONS

We have modeled the response of anatase titania to biaxial strain with emphasis on the change in band gap and charge carrier effective masses. Now, we briefly consider how pressure-induced band gap reduction may be expected to affect the solar-to-hydrogen conversion efficiency. Integration of the solar irradiance data[42] finds the maximum possible absorption dependence on the band gap. For the generally accepted 3.2 eV experimental value for anatase titania, this leads to only about 3.7%. Therefore, even a perfect photon conversion efficiency yields an inadequate solar-to-hydrogen conversion. Using our calculated slope of 68.5 meV/GPa allows us to plot the maximum achievable efficiency vs the total pressure, as shown in Fig. 5. Due to the shape of the solar spectrum in this energy range, the linear change in the band gap leads to an exponential dependence between efficiency and total pressure. We therefore believe that strain-induced band gap reduction will allow anatase titania to achieve a practical solar-to-hydrogen conversion efficiency.

ACKNOWLEDGMENTS

Funding for this work was provided by the Basic Energy Sciences Office, U.S. Department of Energy, under Grant No. DE-FG02–05ER46254. The ABINIT code is a common project of the Université Catholique de Louvain, Corning Inc., and other contributors (http://www.abinit.org).

[1] T. Bak, J. Nowotony, M. Rekas, and C. C. Sorrell, Int. J. Hydrogen Energy **27**, 991 (2002).
[2] H. Tang, K. Prasad, R. Sanjinés, P. E. Schmid, and F. Lévy, J. Appl. Phys. **75**, 2042 (1994).
[3] C. Xu and S. U. M. Khan, Electrochem. Solid-State Lett. **10**, B56 (2007).
[4] T. Okato, T. Sakano, and M. Obara, Phys. Rev. B **72**, 115124 (2005).
[5] M. Radecka, K. Zakrzewska, M. Wierzbicka, A. Gorzkowska, and S. Komornicki, Solid State Ionics **157**, 379 (2003).
[6] M. Radecka, M. Wierzbicka, S. Komornicki, and M. Rekas, Physica B (Amsterdam) **348**, 160 (2004).
[7] G. Zhao, H. Kozuka, H. Lin, M. Takahashi, and T. Yoko, Thin Solid Films **340**, 125 (1999).
[8] B. J. Van Zeghbroeck, Principles of Semiconductor Devices, Sec. 2.3.3.3, Aug 2007 (http://ece-www.colorado.edu/~bart/book/).
[9] J. Guerra, U.S. Patent Application No. 10/424,259 (April 2003).
[10] K. Rajeshwar, in *Encyclopedia of Electrochemistry*, edited by S. Licht (Wiley, New York, 2002), Vol. 6, Chap. 1, p. 24.
[11] X. Gonze, G.-M. Rignanese, M. Verstraete, J.-M. Beuken, Y. Pouillon, R. Caracas, F. Jollet, M. Torrent, G. Zerah, M. Mikami, Ph. Ghosez, M. Veithen, J.-Y. Raty, V. Olevano, F. Bruneval, L. Reining, R. Godby, G. Onida, D. R. Hamann, and D. C. Allan, Z. Kristallogr. **220**, 558 (2005); A brief introduction to the ABINIT software package.
[12] W. G. Aulbur, L. Jonsson, and J. W. Wilkins, Solid State Phys. **54**, 1 (2000).
[13] M. S. Hybertsen and S. G. Louie, Phys. Rev. B **34**, 5390 (1986).
[14] R. W. Godby, M. Schluter, and L. J. Sham, Phys. Rev. B **35**, 4170 (1987).
[15] M. Rohlfing, P. Kruger, and J. Pollmann, Phys. Rev. B **48**, 17791 (1993).
[16] Opium-Pseudopotential Generation Project (http://opium.sourceforge.net/).
[17] J. P. Perdew, K. Burke, and M. Ernzerhof, Phys. Rev. Lett. **77**, 3865 (1996).
[18] H. J. Monkhorst and J. D. Pack, Phys. Rev. B **13**, 5188 (1976).
[19] C. G. Broyden, J. Inst. Math. Appl. **6**, 222 (1970).
[20] R. Fletcher, Comput. J. **13**, 317 (1970).
[21] D. Goldfarb, Math. Comput. **24**, 23 (1970).
[22] D. F. Shanno, Math. Comput. **24**, 647 (1970).
[23] F. Birch, Phys. Rev. **71**, 809 (1947).
[24] M. Calatayud, P. Mori-Sanchez, A. Beltran, A. M. Pendas, E. Francisco, J. Andres, and J. M. Recio, Phys. Rev. B **64**, 184113 (2001).
[25] G. Cangiani, Ph.D. thesis, Ecole Polytechnique Federale De Lausanne, 2003.
[26] M. Mikami, S. Nakamura, O. Kitao, H. Arakawa, and X. Gonze, Jpn. J. Appl. Phys., Part 2 **39**, L847 (2000).
[27] R. Asahi, Y. Taga, W. Mannstadt, and A. J. Freeman, Phys. Rev. B **61**, 7459 (2000).
[28] S.-D. Mo and W. Y. Ching, Phys. Rev. B **51**, 13023 (1995).
[29] A. Fahmi, C. Minot, B. Silvi, and M. Causa, Phys. Rev. B **47**, 11717 (1993).
[30] R. M. Martin, *Electronic Structure: Basic Theory and Practical Methods* (Cambridge University Press, Cambridge, 2004), Chap. 2, p. 44.
[31] L. J. Sham and M. Schluter, Phys. Rev. Lett. **51**, 1888 (1983); Phys. Rev. B **32**, 3883 (1985).
[32] M. Stadele, M. Moukara, J. A. Majewski, P. Vogl, and A. Gorling, Phys. Rev. B **59**, 10031 (1999).
[33] M. Ali Omar, *Elementary Solid State Physics* (Addison-Wesley, Reading, MA, 1993), Chap. 5, p. 229.
[34] J. K. Burdett, T. Hughbanks, G. J. Miller, J. W. Richardson, Jr., and J. V. Smith, J. Am. Chem. Soc. **109**, 3639 (1987).
[35] T. Arlt, M. Bermejo, M. A. Blanco, L. Gerward, J. Z. Jiang, J. S. Olsen, and J. M. Recio, Phys. Rev. B **61**, 14414 (2000).
[36] V. Swamy and L. S. Dubrovinsky, J. Phys. Chem. Solids **62**, 673 (2001).
[37] M. Lazzeri, A. Vittadini, and A. Selloni, Phys. Rev. B **63**, 155409 (2001).
[38] J. Muscat, V. Swamy, and N. M. Harrison, Phys. Rev. B **65**, 224112 (2002).
[39] A. Stashans, S. Lunell, and R. W. Grimes, J. Phys. Chem. Solids **57**, 1293 (1996).
[40] J. R. Simpson, H. D. Drew, S. R. Shinde, R. J. Choudhary, S. B. Ogale, and T. Venkatesan, Phys. Rev. B **69**, 193205 (2004).
[41] M. Stamate, G. Lazar, and I. Lazar, Rom. J. Phys. **53**, 207 (2008).
[42] ASTM International, Designation: G 173-03, 2006.